



Estd. 1989

JOURNAL OF ULTRA SCIENTIST OF PHYSICAL SCIENCES
 An International Open Free Access Peer Reviewed Research Journal of Mathematics
 website:- www.ultrascientist.org

Absolute temperature directly from plank's profile: A simulation

V. VIJAYAKUMAR

B-111, Saivihar, Sector-15, CBD-Belapur, NaviMumbai-400614 (India)

Corresponding Author Email:- drvviyakumar@gmail.com

<http://dx.doi.org/10.22147/jusps-A/330201>

Acceptance Date 18th February, 2021,

Online Publication Date 24th February, 2021

Abstract

The measured thermal radiation from a material surface will, in general, have a wave length (λ) dependent scale-factor to the Planck profile (P_T) from the contributions of the emissivity (ϵ_λ) of the surface, the response function (A_λ) of the measurement setup, and the emission via non-Planck processes. For obtaining the absolute temperature from such a profile, a procedure that take care of these dependencies and which relay on a temperature grid search is proposed. In the procedure, the deviation between the Planck profiles at various temperatures and the measured spectrum that is made equal to it at a selected wavelength, by scaling, is used. The response function (A_λ) is eliminated at the measurement stage and the polynomial dependence of the remnant scale factor mostly dominated by ϵ_λ is extracted from the measured spectrum by identifying its optimal λ dependence. It is shown that when such a computation is carried out over a temperature grid, the absolute temperature can be identified from the minimum of the above deviation. Here, search for T and ϵ_λ delinked, unlike in the least-square approaches that are normally employed. Code that implements the procedure is tested with simulated Planck profile to which different viable values of ϵ_λ and noise is incorporated. It shown that if the λ dependence of scale-factor is not too high, the absolute temperature can be recovered. A large λ dependent scale-factor and the consequent possible error in the temperature obtained can also be identified.

Key words : Planck profile, Absolute Temperature scale, Temperature measurement

Introduction

The temperature scale and its measurement is based on the suggestion¹ that assigned fixed points and a prescription to interpolate between those, be used to establish a practical temperature scale. The ITS-90 scale based on international agreement on the specification of the methods for calibrating several kind of

'thermometers' in a way to make the results repeatable and compatible, at all temperature regions and in different methods of measurements, is based on this approach. It specifies the material properties to be used at several points where temperature can be held constant and assigned values, cross checked and altered, if necessary. There are accepted functions and methods for interpolation between these points. The reference temperature points employed in ITS-90^{2A,B,3}, are at the melting / triple points of pure or mixture of materials. Such points can be identified and temperature at that point held constant utilizing the thermal arrest due to the co-existence of phases even when the temperature is unknown; T is assigned in a consistent / agreed manner as mentioned above. The extension of the scale^{4,5}, to higher temperatures is carried out by measuring the optical power of emission from a defined surface area and in a chosen narrow wavelength band by filter radiometer⁶ at newly identified fixed points. A calibration procedure and specialized experimental set up are used^{5,6}. The temperature is obtained from a least square fit of the observed and computed power by the integration of the Planck profile over a small selected wavelength region. The fact that this uses typically only a very small part of the Planck profile and other considerations necessitate correction to be added to the inferred temperature points^{5,7}. With three or more points so obtained, Sakumata-Hattori-function⁸ is used for further refinement and for interpolation between the points. Thus this and an alternate approach⁹ emphasize on reproducibility and traceability but do not use the Planck profile directly, nor the dependence of emissivity on temperature and wavelength properly taken care off. Thus an approach that do not require temperature at fixed points to be pre-assigned a value, prescriptions for interpolation, do not collect extraneous signals (from a surface) and employs the Planck's profile directly, taking care of the dependence of emissivity on material phase, temperature and wavelength, is desirable for establishing the absolute temperature points and a scale.

The Planck radiation profile derived on the basis of the basic physical laws (quantum principles that decide the allowed photon states and its occupation as per the Boltzmann distribution) for a 'black body' is material independent and should be exclusively employed to establish the absolute temperature scale. The idealized situation (i.e. material independence) of a radiation source is obtained in a 'black body' (a large cavity kept at constant temperature)¹⁰, as it can be reasonably made to satisfy the assumptions employed in the derivation of the Planck profile. For practical reasons, a container with the required materials to identify the temperature point inside it is kept within the cavity and the radiation from the container surface is employed. The photons collected from container surface will originate from a thin volume (that imitate a cavity) near the surface and will undergo self-absorption within its volume, and refraction and scattering at the interface, in a λ dependent way. Thus the spectral intensity irradiated by the surface is a Planck distribution scaled in a λ and material phase dependent way, justifying the use of emissivity (ϵ_λ) as a scale-factor to Planck's profile. A spectrograph that rejects stray signals can yield such a thermal radiation profile. However the measured profile will be distorted due to the λ dependent response factor (A_λ) of the measuring setup; i.e. the electronic amplification, the wavelength dependent efficiency of the detector, and the deleterious effects of chromatic aberration / refraction in the optical elements etc.. Thus the measured profile counts C_λ at a temperature T will have a composite scale-factor, S_λ , to the Planck profile (P_T) as:-

$$C_\lambda = S_\lambda P_T \quad \text{I}$$

$$\text{With } P_T = \lambda^{-5} / [e^{(S_2/\lambda T)} - 1],$$

and $S_2 = 1.43877 \times 10^7$ (nm.K) and $S_\lambda = \epsilon_\lambda A_\lambda$ with $S_1 = [3.74177 \times 10^8 \text{ (W}\mu\text{m}^4/\text{m}^2)]$ absorbed in A_λ .

This composite scale-factor, S_λ that has wave length dependence, is the impediment in establishing a

temperature scale and its measurement using a measured profile directly. It may be noted that any non-Planck process, and it will be present because of the self-absorption and re-emission, will further modify this scale-factor.

In comparison to establishing temperature scale by the fore-mentioned approaches, multi-wavelength thermometry aims to determine both, temperature and S_λ simultaneously employing equation-I from the measured spectral radiance at several (say N) wavelengths. There are N measured values and N+1 unknowns (NS_λ values plus temperature). There are several approaches¹¹; the obvious one is to assume or obtained via calibration, the values of the N combined scale factors. If for a spectra, temperature, T, is known or assigned a value (what is normally done), then N different factors by which the observed N intensities needs be multiplied to convert the observed spectra to the Planck's profile can be obtained and employed for the determination of any other temperature. Additional simplifying assumption like that this scale factor is same at two (or more) agreed wavelengths makes the procedure easy. Thus the temperature may be obtained in a reproducible manner from the ratio of intensities at selected wavelengths, employing equation-I. This "effective" temperature is indeed dependent on the wavelengths chosen and details of S_λ . Thus, all these aspects need to be specified and followed in all measurements. Another approximation is to assume S_λ is a polynomial in λ , reducing the number of unknowns (four in the case of a third order polynomial) and then carryout a least square refinement. However, strong correlation between the coefficients of S_λ and T will result in divergence problems and most often one have to resort to a grey body approximation. A delinking of T and the polynomial coefficients (apart from reducing these as much as possible) is a viable solution to get temperature on an absolute scale and avoiding the *ad hocism and error proneness*.

Absolute temperature points recovery :

For recovery of absolute temperature corresponding to a profile, a procedure that employ a spectrum that is corrected for the usually large λ dependent response function, A_λ , of the measuring set up, is considered. Correcting for the response function is not a serious constraint, as it can be accurately measured by monitoring the output when the same fixed number of photons of various wavelengths is used as input. For such a corrected spectrum (λ vs C_λ), the equation I may be rewritten as:-

$$\epsilon_\lambda = C_\lambda / P_{T1} \quad \text{II}$$

ϵ_λ in II represents the scale-factor and has contribution mostly from the emissivity of the surface from which the radiation is collected. In the following discussion, as the response function has been compensated, emissivity and scale-factor are used interchangeably. Before proceeding further, the nature of variation of ϵ_λ needs to be examined. The easily measurable surface reflectivity, r, ($\epsilon_\lambda = 1-r$), and a comparison between spectral radiation intensities measured from a material and a blackbody, are usually used to measure emissivity (ϵ_λ) as an intrinsic property¹². In the latter case, the accuracy of the measured ϵ_λ is independent of the temperature value assigned at the measurement point unlike the former case where it depends on the value assigned to the black body. Measurements on typical metals like Zr, Rh¹³, Ni¹⁴, W, Ta¹⁵, Nb¹⁶ etc. show a smooth negative dependence of ϵ_λ as expected from the fact that the dominant physical process that the emitted radiation undergo is self-absorption. A material, ZrC¹⁷, with a high melting point shows a relatively small dependence of ϵ_λ on λ . Another interesting case is that of graphite nanostructure which has a constant ϵ_λ close to 0.99 over

a wide λ and temperature range¹⁸ and can be treated as a black body (BB) surface. Thus ϵ_λ data typically varies smoothly with λ and may be represented by a polynomial in λ ¹⁷.

In the following, assuming a polynomial dependence of ϵ_λ on λ , an approach that can surmount limitations in establishing the absolute temperature scale is proposed.

With a polynomial approximation of ϵ_λ , II can be written as:-

$$C_\lambda/P_{T1} = \epsilon_\lambda = \epsilon_0[1 + a\lambda + b\lambda^2 + c\lambda^3 + \dots] \quad \text{IIA}$$

where ϵ_0 is the λ independent part of ϵ_λ and a, b, c etc. are the material phase, temperature, and pressure and λ dependent coefficients of the polynomial. A scaling of the counts C_λ by a factor F_a (or the mathematically equivalent multiplication of P_{T1} by F_a) that equalizes the computed and observed count at a particular wavelength, λ_1 (ie. $F_a = C_{\lambda1}/P_{T\lambda1}$; $P_{T\lambda1}$ is the value of P_{T1} at the wave length λ_1) will eliminate any constant multiplier / scaling (the λ independent signal amplification and ϵ_0) in the measured spectra and has a further utility as will be clear from the discussions to follow. Though λ_1 can be any wavelength with in the spectral range of the profile, here (in the codes used in simulations) the wavelength at the middle of the spectral region is used.

Thus, IIA with the scaled emissivity, $C_{s\lambda}$, takes the form:-

$$C_{s\lambda}/P_{T1} = \epsilon_{s\lambda} = [1 + a\lambda + b\lambda^2 + c\lambda^3 + \dots]/[1 + a\lambda_1 + b\lambda_1^2 + c\lambda_1^3 + \dots] \quad \text{IIIA}$$

This scaling when repeated with a profile at any other temperature, T_g , gives a quantity $\epsilon_{g\lambda}$, related to $\epsilon_{s\lambda}$ as:-

$$\epsilon_{g\lambda} = C_{s\lambda}/P_{Tg} \quad \text{IIIB}$$

$$\text{ie. } \epsilon_{g\lambda} = [P_{T1}/P_{Tg}] C_{s\lambda}/P_{T1}$$

$$\text{Thus, } \epsilon_{g\lambda} = [P_{T1}/P_{Tg}] \epsilon_{s\lambda} \quad \text{IIIC}$$

When the grid point (T_g) coincides with true temperature, T_1 , $[P_{T1}/P_{Tg}]$ will be equal to one. It will be λ dependent and less or greater than unity depending on whether T_g is greater or less than T_1 . Again, from III-A & C it is evident that if $\epsilon_{g\lambda}$ is computed and fitted to a polynomial over a temperature grid that encloses T_1 , as one move away from T_1 , higher and higher degree polynomial will be required for fitting it. This follows from the fact that $[P_{T1}/P_{Tg}]$ is approximately an exponential function of ΔT , the deviation of the grid point from the actual temperature. If a constant polynomial degree (equal to or lower than the actual λ dependence of $\epsilon_{s\lambda}$ at T_1) is used at all grid points then, from III-B, μ ($\mu = \sum (C_{s\lambda} - \ddot{E}_\lambda P_{Tg})^2$; the summation is over the discrete wavelengths of the spectrum and \ddot{E}_λ is the emissivity recomputed from the fit of $\epsilon_{g\lambda}$ to a polynomial of the selected constant degree) will have a minimum at the correct temperature. It will increase as the grid point moves away, because of the increasing misfit. This will happen as long as the change in λ variation of $\epsilon_{s\lambda}$ with temperature is lower than that of $[P_{T1}/P_{Tg}]$ as evident from IIIC. This fixes the range of λ variation of the scale-factor that can be tackled by this procedure. At T_1 , the λ independent part of the scaled emissivity ($\epsilon_{s\lambda}$) will

approach unity if the ϵ_λ have only weak λ dependence (a, b, & c close to zero in Eq IIIA). Thus, μ minimum can be employed to get the correct temperature and the deviation of the λ independent part of $\epsilon_{s\lambda}$ at the μ minimum from unity, to judge the extent of the remnant λ dependence of ϵ_λ . If, $\mu'[\mu' = \sum(C_{s\lambda} - P_{TG})^2]$, i.e. $\ddot{E}_\lambda = 1$ corresponds to emissivity when a, b, c etc. are all zero & ϵ_0 equal to one] is computed, temperature under grey body approximation can also be identified.

Simulations :

To check the approach, simulated profiles (employing a code `planck-p`¹⁹) with different parameters (T, ϵ_0, a & b), slightly λ dependent step seize, and various noise levels, in several spectral regions, are generated and used. The pre-peak spectral region of Planck's profile has the steepest positive gradient (in contrast to the negative gradient of emissivity), and as mentioned earlier, will be better suited for a successful application of the method. With `planck-p`, simulated profiles can be generated with any starting point and spectral width. For the results discussed in detail here (Fig I A & B and Table I), a spectral width of 1000 nm with, a starting point where the count is about 50 when the highest count is constrained to be between 6×10^4 to 10^6 , as in a typical measurement, is used. This is done by scaling the profile and or shifting the starting point.

Material	λ_{st}	ϵ_0	a	b	ϵ_λ Range	T_s K	D	$\epsilon_{s\lambda}^0$	T_r K	\square	T_{gr} K
C[18]	810	.99	0	0	.8-.8	1600	1	.9971	1600	0.	1600
Ta[14]	810	.624	.1913	-.2634	.614-.162	1600	3	1.520	1597	-3	1797
W[14]	810	.5421	-.1756	.0083	.464-.335	1600	2	1.566	1605	+5	1758
Ni[13] ⁺	670	.2311	.3904	-.3411	.412-.005	1728	3	1.08	1724	-4	2406
Mo[14]	300	.4971	.3715	-.3621	.575-.368	2500	3	.889	2499	-1	2502
Nb(l)[16]	260	.3899	-.0691	.00504	.372-310	2750	2	1.128	2752	+2	2796
W[14]	260	.5032	-.1542	.0168	.464-.335	2800	3	1.272	2801.5	1.5	2965
ZrC(s) [17]	240	.6968	-.2752	.164	.687-.553	3155	3	1.747	3154.5	-.5	3127
ZrC(l) [17]	240	.8666	-.8678	.4961	.642-610	3155	3	1.194	3154.5	-.5	3223
GB	240	.7	0	0	.9-.9	3155	1	.9993	3155	0.	3155
*	240	.1	.3	.2	.183-.778	3155	3	.256	3152.5	+2.5	2789

Table I :- Typical runs for identifying absolute temperature. Literature data on ϵ_λ for the listed materials, a gray body (GB) and a case of monotonic increase (*) that do not correspond to any material are listed. The emissivity range covers different variation types; constant, monotonic decrease, minimum (ZrC), and monotonic increase. The coefficients, ϵ_0 , a and b (c=0 not shown), correspond to the case where λ is in micron. For simulations for Ta(1600K) & Mo(2500K), reflectivity data reported at 300K is used for getting ϵ_λ . λ_{st} is the optimal starting point of the spectral region used and have a value that varies between 810 and 200 nm depending on the temperature. T_s , T_r , & T_{gr} respectively are the simulation, recovered, and the grey body temperature. $\epsilon_{s\lambda}^0$ is the λ independent part of scaled emissivity given by equation IIIA. \square is the difference between the simulation and recovered temperatures. A polynomial order lower by one as compared to the value used in the simulation is recovered for W (1600K) and Nb because the 'b' value is small and the procedure gives a preference to a lower poly order.

This ensures that at low temperature or λ , the counts are not too low and the generated spectrum covers the pre-peak and peak region of the profile optimally. Such starting point depends on the temperature and planck-p can locate it. Tests have also been carried out with two other fixed starting points 600 and 400 nm, both with different spectral widths (500 /750 /1000 nm). For spectral width lower than 500 nm the procedure works better if the pre-factor is almost λ independent. The spectral width of 1000 nm is optimal to avoid error in the recovered temperature even in presence of anomalous λ dependence (maximum/ minimum or large variation) of emissivity / pre-factor and in any spectral region. Instead of using arbitrary values the coefficients (ϵ_o , a & b), those of some materials listed in Table I is used. Thus the requirement that ϵ_λ needs to be positive in the spectral region considered and should mostly decrease with increasing λ as indicated by the measured emissivity is met. This not only tests the procedure described here but will also demonstrate how it will perform in practice. The scaled Planck profile is multiplied by ϵ_λ and random numbers of magnitude, within a choose-able limit ($=F \times N$, N, square root of the count, F a random fraction between -1 and 1) is added as noise, only after its scaling mentioned above. This ensures that scaling do not dilute the effect of noise and ϵ_λ in the final profile. A background is also generated and added to the profile to imitate the dark noise of a detector. The profile and the background are stored in separate files. This is to enable subtraction of the separately measurable dark noise while processing measured data. Thus with a slightly unequal step seize in λ , added noise, provision to remove dark noise of the detector, and ability to choose a convenient spectral region with sufficient counts, the simulated data used in testing mimics a typical measurement well.

For extracting absolute temperature from the simulated profiles, a code (a-temp¹⁹ that will generate temperature grid points, T_g , ($T_g = T_i \pm \partial$, ∂ varies in steps of 0.5 K from $-\partial$ to ∂ ; T_i is a trial temperature that differ from real temperatures T_1 by a maximum of $\pm \partial$) and compute at each grid point, $\epsilon_{g\lambda}$, μ and μ' is used.

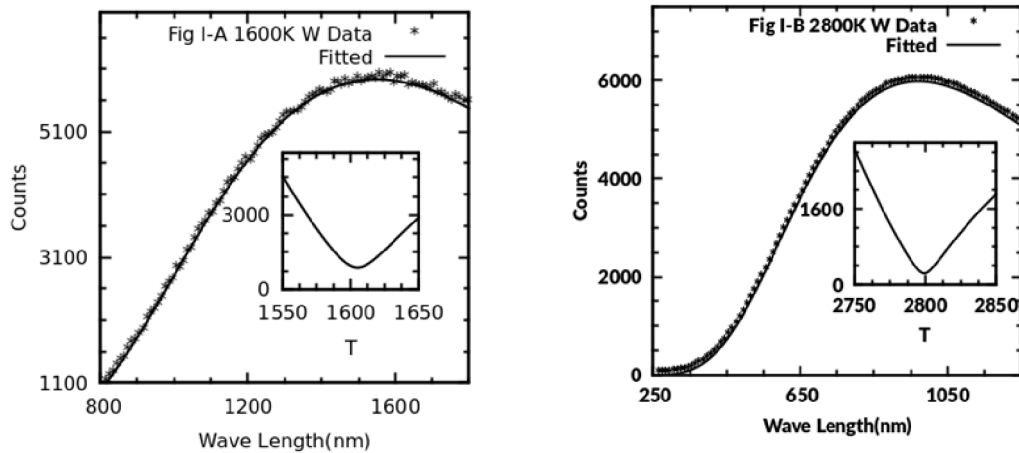


Fig I Results of the procedure to identify absolute temperature for W at two temperatures. The insert is the variation of μ in the ± 50 K region of the recovered temperature. The search region can be increased to ± 1400 or more (depending on temperature) without any divergence problem and thus effectively no information on T or remnant scale factor (guess or preassigned) required. Details of all the simulations discussed in the text are included in the Table I

While dealing with measured spectra no information on the λ dependence of remnant ϵ_λ will be

available and hence the issue as to how to pre-decide which polynomial order is to be employed while analyzing the data needs to be solved. This is addressed by comparing the values of $D\mu$ (D, square root of the order of the polynomial) for various values of D and accepting the polynomial order that gives the lowest $D\mu$, at each grid point. This may lead to a preferential selection of a lower order polynomial, but this decision is based on an 'estimate' from the data and consistent with the requirement of the procedure. In all tests carried out, this approach correctly recovers the polynomial order used in the simulation unless the coefficients of the highest power in λ are very small. In such cases, a polynomial order lower by one as compared to the value used in simulation is recovered. But such lower polynomial order does not result in any large variation between the recovered temperature and that used in simulation. To retain flexibility, a-temp can pre-assume a particular fixed polynomial order for all grid points or search and identify a polynomial order that has lowest $D\mu$ at each grid point, in two separate mode of operation. Keeping in view of measurement situation, it also incorporates a Savitzky-Golay Filter²⁰ to eliminate the random fluctuations in the profile. Up to ten temperature pairs for which μ is low and arranged in its increasing magnitude is stored to check whether the minimum in μ is approached monotonically and how far the λ independent part of $\epsilon_{s\lambda}$ is different from unity. This enables checking whether the accuracy of T_1 is compromised by a large λ dependence (magnitude do not affect accuracy because of the scaling used) of $\epsilon_{s\lambda}$. The monotonicity of μ will be broken if there is too much noise in the spectra or an inappropriate polynomial order gets selected (as inferred from the few of theseveral simulations) because of the peculiarities / wiggles in the λ dependence of $\epsilon_{g\lambda}$. If the trial temperature is too far from the correct temperature, the λ independent part of $\epsilon_{s\lambda}$ will substantially deviate from unity (because $\epsilon_{g\lambda} = \epsilon_{s\lambda} [P_{Tg}/P_{T2}]$) and also there will not be any μ minimum. A-temp detects such error conditions and will suggest whether to increase the error range / change the trial value of temperature, or use an appropriate constant polynomial order. It may be noted that unlike in a nonlinear least square procedure, no guess values of T, ϵ_0 , and the order and the coefficients of the $\epsilon_{s\lambda}$ polynomial, needs to be provided and procedure works even for a large search region of T. For example if T is 1600, one can search 200 -3000 region and locate the correct value.

In simulations, the computation of μ is initially carried out for various orders of the polynomial and the grid point (temperature) and polynomial order that gives minimum in $D\mu$ is identified. The computations are then repeated with the identified or the next higher polynomial order. In such re-computations, a higher polynomial order is employed only if the lower one results in a non-monotonic variation of μ with T (none of the cases listed in table I needed this). This is justified because the procedure to identify D gives an over weightage to a lower order polynomial as indicated earlier. Results listed in Table I, uses simulated spectra with listed polynomial coefficients for emissivity and added maximum noise of $\pm 0.5F \times N$. Result of typical runs for a black body (BB) imitating graphite nanostructure (1600), grey body(3155 K), W (1600 & 2800 K), Ta (1600 K), Nb (2750 K), and ZrC (3155 K for melt and solid data) are summarized in Table I. Typical result of fitting for W is shown in fig IA & B. The temperature points used are dictated by the available data on $\epsilon_{s\lambda}$ and do not have any other significance. $\epsilon_{s\lambda}$ data available as tabulation (Ta & W) has been fitted to a polynomial and the coefficients used. Table I also lists a case where the emissivity monotonically increases with temperature and do not represent any material. Several other simulations were made successfully, but are not discussed here.

From the results of simulations (listed in Table I & several others), the following conclusions are reached. It may be noted that the accuracy of the procedure is indicated by how far the recovered temperature is different from that used in simulating the profile. The monotonic variation of μ over the grid and closeness of $\epsilon_{s\lambda}^0$ to unity is how the accuracy of recovered temperature needs to be accessed. The μ value have the steepest variation, lowest value at its minimum and the recovered temperature closest to that used for simulation, for graphite nano structure and grey body (GB) profiles (Table I). Here, $\epsilon_{s\lambda}^0$ is close to unity at the correct

temperature irrespective of the magnitude of ϵ_0 used in simulation. Though at the minimum of μ , a polynomial order of one is detected, as one moves away from the temperature value used for simulation, $\epsilon_{s\lambda}$ gets fitted to polynomials of higher and higher order as expected from III-C

Other cases listed are those with a various kind of λ dependence of ϵ_λ .

Ta & Nb have a small value for the coefficient b for ϵ_λ .

Thus, for Nb, a polynomial order of two (instead of three) is detected but the temperatures are recovered.

Widely used W has an emissivity that decreases steeply over the spectral region considered. There is relatively large error in temperature recovered especially at low temperature (1600 K) where a lower polynomial of order two is identified.

Ni represents a case in which the emissivity varies over a large range. Consequently, the recovered temperature has larger errors

In ZnC, the emissivity has only a small variation and hence temperature and polynomial degree are recovered.

In the case of a positive temperature gradient also temperature and polynomial order is recovered.

In the above last five cases, the λ independent part of $\epsilon_{s\lambda}$ deviates from unity at the minimum of μ . But it is seen that for small such deviation, the correct temperature is still recovered. The extent of deviation of the λ independent part of $\epsilon_{s\lambda}$ from unity indicates the extent of the λ dependence of ϵ_λ and possibility of error in the recovered temperature. It should be noted that if the spectrum is collected from a carbon nano surface with a fully A_λ compensated setup, a D and $\epsilon_{s\lambda}^0$ close to one will be identified and in such a case, the ϵ_λ used here demonstrate the tolerance of the procedure to the presence of stray signals in such a measurement. Thus if one uses nano-structured graphite as a temperature marker, the method will work even when there is small remnant λ dependence of pre-factor in the measured spectra. Such dependence can originate from the intrinsic emissivity of the surface, the error in the elimination of spectral response of the system, and the existence of non-Planck processes, all of which cannot be identified and removed at the time of measurement.

The grey body temperature, as expected, is very different, from absolute temperature (except for BB) with the deviation decided by the extent of λ dependence of ϵ_λ . For a negative λ dependence of ϵ_λ that is normally found, under the grey body approximation, the temperature is overestimated.

The effect of added noise was also checked [not listed in the table I], and as expected, increasing noise level resulted in an overall increase in μ . For moderate noise levels (detectable at the filtration stage) there is no shift in μ minimum. For large noise levels, a non-monotonicity in the variation of μ over the temperature grid and shifts in minimum is observed. This error condition which needs to be eliminated at the measurement stage will be detected by a-temp. The noise level used in the simulations here is enough to correspond to a typical measurement condition.

In addition to noise, the procedure should be unaffected by other interferences also. The effect of the uncertain ϵ_λ of the material surfaces due to non-intrinsic factors like surface creep, texture/roughness, formation of over-layers (oxides/nitrides) etc. needs consideration. These, when present, can make ϵ_λ value somewhat heating history and time dependent. Also these can scatter the emitted radiation and vary the 'effective' ϵ_λ with time in a random way during data collection. Several thermal cycling of the surface prior to the actual measurement and keeping the material in inert atmosphere will alleviate this problem to a large extent. In the

Planck profile, ϵ_λ appear as a scaling factor. Thus the random variations in ϵ_λ can be replaced with an effective (time averaged) $\bar{\epsilon}_\lambda$, provided the spectra over the entire λ band employed is acquired simultaneously with an area detector. Since the procedure described here does not need any prior knowledge of the magnitude or λ dependence of emissivity, it will work even in presence of such an averaging. In measurements, it is indeed observed that such random variations in emissivity do not affect the inferred temperature²¹. Since the λ dependence of emissivity and not its magnitude that decide the accuracy of recovered temperature, it will be desirable to reduce such dependency as much as possible. In this context, the large and the almost λ independent throughput over a wide wavelength region and non-corruption by higher order diffraction, is a clear reason to favor a prism based spectrometer. This along with an area detector and con-focal input optics will enable successful application of the method discussed here. If the non-Planck processes give only a smoothly varying background, it will get absorbed in the polynomial dependence of scale-factor and is already taken care off in the procedure. Thus with carefully conducted experiments the absolute temperature can be extracted without any pre-assigned fixed points even in presence extraneous contributions. The envisaged procedure will still use cavities with appropriate material corresponding to a temperature point inside a container to which a temperature marker is also attached. Thus cavity's role is to ensure constancy of temperature while the spectrum is being collected from the temperature marker.

Conclusions

If the response function of a setup can be independently measured, then a profile measured from any material whose emissivity is a smoothly varying function of λ can be used to obtain the corresponding absolute temperature. It is better to use a prism based setup for measurements because of the low λ dependent A_λ and non-interference from higher order diffraction. In such a case, the elimination of A_λ may not be necessary. Thus, it is possible to establish the absolute temperature scale without any assigned fixed points and interpolation/extrapolation procedure. This requires no trial values of emissivity to be known as it is 'estimated' from the data itself; there is a matrix for judging the accuracy of the recovered temperature. There is a complete decoupling in identifying the λ dependence of $\bar{\epsilon}_\lambda$ and the temperature so that problem of divergence is eliminated and full range of temperature can be scanned to identify the correct temperature. Also it is established that the accuracy of the recovered temperature do not depend on the magnitude of the emissivity but only on its wavelength dependence thus reducing the role of cavities only to provide constancy of temperature. Thus the criticism²² of employing cavities as black body standards becomes irrelevant. It may be mentioned that based solely on Planck's profile, any arbitrary temperature can also be identified if the marker is attached to a large thermal mass so as to have a constant temperature during measurements.

The requirement that the spectral response of the system should be independently measured is an impediment for the routine use of this approach. Thus it is useful to investigate whether the procedure can be extended to systems with unknown response. Indeed, if T_1 is a temperature identified as per the procedure, a re-measurement of the profile, P_{T_1} , at T_1 with a system of unknown response can be used to identify any temperature, T_2 , that corresponds to any other profile, P_{T_2} , measured with the same setup. This extension of the approach will be similar to the calibration procedure¹¹ and will be addressed in a subsequent publication.

Data Availability :

The data used in this study are available from the author upon request / from googledrive link¹⁹.

Funding :

No funding support from any agency was sought or received for this work.

References

1. H. L. Callendar, *Phil. Mag.* Vol 48, Page 519-547 (1899)
- 2A. H. Preston-Thomas. (1990); *Metrologia*, Vol 27, Page 3-10.
- 2B. H Yoon, P Saunders, G Machin, A D Todd, Guide to the Realization of the ITS-90 Radiation Thermometry, <https://www.bipm.org/utils/.../ITS-90/Guide-ITS-90-RadiationThermometry-2017.pdf>
2C/B Fellmuth, E Mendez Lango, T Nakano, F Sparasci, Guide to the Realization of the ITS-90 Cryogenic Fixed Points, <https://www.bipm.org/utils/.../ITS-90/Guide-ITS-90-Cryogenic-Fixed-Points-2017.pdf>
3. H. W. Yoon, V. B. Khromchenko, G. P. Eppeldauer, C. E. Gibson, J. T. Woodward, P. S. Shaw and K.R. Lykke, *Phil.Trans.R.Soc.A374*: 20150045, <http://dx.doi.org/10.1098/rsta.2015.0045> (2016).
4. Woolliams. E.R *et al.*, *Phil. Trans.R. Soc.A374*:20150044 (2016). <http://dx.doi.org/10.1098/rsta.2015.0044>
5. Fellmuth. B, Fischer. J, Machin. G, Picard. S, Steur. P.P.M, Tamura.O, White. D.R, Yoon. H., *Phil. Trans. R. Soc. A 374*: 20150037 (2016); <http://dx.doi.org/10.1098/rsta.2015.0037>
6. Jürgen Hartmann, *Int J Electrical and Computer Engineering Systems*, Vol 5, Pages 63-67 (2014).
7. E.R. Woolliams, *Int J Thermophysics Vol 35* (6–7), Page 1353-1365 (2014).
8. https://en.wikipedia.org/wiki/Sakuma%E2%80%93Hattori_equation
9. A. Prokhorov V. Sapritsky · B. Khlevnoy · V. Gavrilov., *Int J Thermophys Vol 36*: Page 252-256. (2015); <https://doi.org/10.1007/s10765-014-1826-7>
10. Robert J. Johnson, *Progress in Physics Vol 12(3)* Page 175-183 (2016).
- 11a). António Araújo, *Meas. Sci. Technol.* Vol 28(8) Page 082002 (2017).
- 11b). H. Jianhui, L. Chong, L. Xiang and Y. Hanyuan, “Data Processing Model of Multi-spectral Thermometry Based on Emissivity Ratio,” *2019 2nd International Conference on Information Systems and Computer Aided Education (ICISCAE)*, Dalian, China, 2019, pp. 452 DOI: 10.1109/ICISCAE48440.2019.221673
- 11c). Daniel Ng and Gustave Fralick, *Rev. Sci. Instruments Vol 72*, Page 1522-1530; <doi.org/10.1063/1.1340558> (2001).
12. Abdelmagid El Bakali, Rémi Gilblas, Thomas Pottier, and Yannick Le Maout, *Rev. Sci. Instrum. Vol 90(11)*, Page 115116 [doi: 10.1063/1.5116425](doi:10.1063/1.5116425) (2019).
13. T. M. Hartsfield, I A. J. Iverson, and J. K. Baldwin, *J. Appl. Phys. Vol 124*, Page 105107 (2018); <https://doi.org/10.1063/1.5042601>
14. Watanabe, H., Susa, M., Fukuyama, H. *et al.*, *Int J Thermophysics Vol 24*: 473-488 (2003); <https://doi.org/10.1023/A:1022924105951>.
- 15a). Russell M. Pon and Jan P. Hessler *APPLIED OPTICS*, Vol 23(7), Pages 975-976 (1984).
b). Jones. JM, Mason. PE and Williams. A, *A compilation of data on the radiant emissivity of some materials at high temperatures.* *J of The Energy Institute*, 92 (3). pp. 523-534. ISSN 1743-9671 (<http://eprints.whiterose.ac.uk/133266/>) (2019).
16. Watanabe, J.T. Okada, M.V. Kumar, P.–F. Paradis and T. Ishikawa, *J. Chem. Thermodynamics*, Vol 91,

- Pages 116-120 (2015).
17. Anatoliy I Fisenko and Vladimir F. Lemberg, *Int. J Thermophysics*, Vol 36, page 2705–2719(2015 DOI: 10.1007/s10765-015-1982-4) & *Int J Thermophysics* Vol 36: Page 1627-1639 DOI: 10.1007/s10765-015-1921-4 (2015).
 - b). Manara D, Jackson HF, Perinetti-Casoni C, Boboridis K, Welland MJ, Luzzi L, Ossi PM, Lee WE., *J European Ceramic Society* Vol 33, Pages 1349-1361 (2013).
 18. Takahiro Matsumoto, Tomoaki Koizumi, Yasuyuki Kawakami, Koichi Okamoto, and Makoto Tomita *OPTICS EXPRESS* Vol 21(25), Page 30964-30974 (2013). DOI:10.1364/OE.21.030964
 19. Codes along with necessary details may be downloaded from:-
https://drive.google.com/drive/folders/12kONEFRJMUZ0xI6RktM_IpkXCfdqcQNY?usp=sharing
 20. For a good description see <http://www.users.waitrose.com/~robinjames/SG/SGhome.html> & https://en.wikipedia.org/wiki/Savitzky%E2%80%93Golay_filter
 21. Maryse Muller and Remy Fabbro, *J of Laser Applications* Vol 24, Page 022006 (2012); <https://doi.org/10.2351/1.3701400>
 22. Robitaille P.M., *Progr. Phys.* Vol 4, Page 3-13 (2009).